inter.noise 2010
noise and sustainability
13-16 June 2010 . Lisbon . Portugal
www.internoise2010.org

Comparison of acoustic single-value parameters for the design process of electrical machines

M. van der Giet[1], M. Müller-Trapet[2]
P. Dietrich[2], M. Pollow[2], J. Blum[1,2]
K. Hameyer[1], M. Vorländer[2]

[1]Institute of Electrical Machines – RWTH Aachen University, Germany
{Michael.vanderGiet@IEM.RWTH-Aachen.DE}
[2]Institute of Technical Acoustics – RWTH Aachen University, Germany
{Pascal.Dietrich@Akustik.RWTH-Aachen.DE}

Abstract
In the development and design process of electrical machines acoustic noise due to the electromagnetic excitation plays an important role. Therefore, designers rely on fast and descriptive scalar parameters to estimate the radiated noise of the machine depending on system parameters, including electromagnetic and structural aspects. Based on a modular approach separating electromagnetic force excitation and transmission by structural dynamics the mean-squared surface velocity over frequency is calculated to assess the acoustic behavior in a simple way. The computational cost can be significantly reduced by using modal superposition of the force excitation and transmission. In order to correlate this simple parameter with the radiated sound power, the latter is calculated based on the complex surface velocity distribution. This is done numerically by boundary element simulations and analytically by decomposition in a set of cylindrical base functions. The analytic calculation is expected to obtain very accurate results for arbitrary receiving points in the acoustic free-field in reduced calculation time making time-consuming BEM simulations unnecessary. Additionally, the time history of the sound pressure at any point can be directly auralized.

Keywords: audible noise of electrical machines, analytical and numerical computation, auralization, modal decomposition.

1 Introduction

Radiated acoustic noise of electrical machines is known and troublesome since many years [1]. The machine designer mainly focuses on the primary functionality of the electrical machine, operating along a specific torque/speed characteristic. Parasitic effects, such as torque ripple, power loss and audible noise are often considered in a second design step. This may lead to unsatisfactory results in terms of acoustic performance.

Due to the trend of increasing electrification of mechanical systems, the increase of power density together with the demand for overall acoustic noise reduction, it is essential to put more focus on acoustic aspects in the development of electrical machines. As the primary force excitation of electrical machines stems from the magnetic field, the designer is concerned with the variation of the magnetic circuit, the winding arrangement, the current supply, etc. to achieve an acoustically optimized design [2]. To assess the effectiveness of a certain electromagnetic design, it is essential to have representative acoustic parameters.

As the transmission path from the electromagnetic (EM) fields and forces leads through the mechanical structure through the surrounding air up to the customer's ears, it is possible to evaluate the design at different levels. For example, force excitations can be compared immediately. If in addition, the structural-dynamic behavior of the machines is analyzed, the vibration in terms of surface velocity can be used as an indicator. Including the radiation problem into the analysis, it is possible to assess the machine design by the sound pressure level at a specific point in space, or to evaluate the total sound power level emitted by the machine. In order not to rely on expensive prototypes and to include acoustic aspects as early as possible in the design process, the acoustic parameters have to be simulated, with as little additional computational effort as possible.

In general, it is possible to address the acoustic problem of electrical machines analytically, or by means of numerical methods. In the first half of the last century, analytical approaches for all three domains: electromagnetic, structural-dynamic and acoustic, were developed [1]. With the upcoming of digital computers numerical techniques became available. Soon a coupling between the Finite Element Method (FEM) and the Boundary Element Method (BEM) became a standard procedure for acoustic analysis of electrical machines [3].

This paper compares different parameters in two different aspects. On one hand, analyzing their precision and significance for the design process and on the other hand their computation time. Based on an exemplarily chosen small electrical machine, the complete simulation chain from EM calculation, over structural FEM, up to the acoustic radiation is processed. The mean-squared normal surface velocity (MSNSV), the sound pressure level and the total radiated acoustic power are calculated. In addition, two different approaches are used to calculate the acoustic field: as a numerical method, the BEM is applied and an analytical model based on cylindrical harmonics is considered as an alternative. A modular simulation concept is applied as proposed by FINGERHUTH ET AL. [4]. This enables parallelization of independent computation tasks leading to shorter calculation times that are expected to be suitable for instant auralization applications in future [5].

2 Electromagnetic-field computation

The most significant excitation of audible noise of electrical machines stems from magnetic forces acting on its stator. Magnetic forces come under volume- and surface-density form. In saturable non-conducting materials, the volume density is basically related to the gradient of the magnetic reluctivity, and it is usually negligible with respect to the surface-force density $\Delta\sigma$. The latter, located at material discontinuities (e.g. on the stator surface in the air gap), is the divergence in the sense of distribution of the electromechanical tensor [6].

Regarding the stator of an electrical machine as a cylinder, electromagnetic forces can be split into two categories: radial and tangential. The radial forces can be evaluated as the surface forces at the interface between the stator and air. They mainly excite the stator structure and lead to vibration. The most relevant effect of the remaining tangential forces is the fact that their integral is the resulting electromagnetic torque, which has a DC component, leading to energy conversion,

and torque harmonics, which may also provoke vibration. A common method to evaluate torque, e.g. from numerical simulation, is to integrate the electromechanical stress tensor in the air gap. This approach is used in this work to obtain the tangential force excitations. For radial-flux rotating field machines in steady state and with time harmonic supply, the radial magnetic flux density $b_{\mathrm{rad}}(x,t)$ at the stator bore can be described by a FOURIER series expansion :

$$b_{\mathrm{rad}}(x,t) = \sum_{\nu=-\infty}^{\infty} \sum_{\mu=0}^{\infty} B_{\nu\mu} \cos(\nu x - \omega_\mu t - \varphi_{\nu\mu}) \,, \tag{1}$$

where x is the spatial angle in the machine, ν and μ are the spatial and temporal harmonic numbers, and $B_{\nu\mu}$ and $\varphi_{\nu\mu}$ are amplitude and phase of the flux-density waves in the air gap of the machine, respectively. The radial surface-force density σ_{rad} at the stator bore is approximated as the radial component of the surface-force density $\Delta\boldsymbol{\sigma}$

$$\sigma_{\mathrm{rad}} = -\frac{b_{\mathrm{rad}}^2}{2\mu_0} \,. \tag{2}$$

Inserting Eq. (1) into Eq. (2) leads to the expression of harmonic radial-force waves

$$\sigma_{\mathrm{rad}}(x,t) = \sum_{r=-\infty}^{\infty} \sum_{m=0}^{\infty} \sigma_{rm} \cos(rx - \omega_m t - \varphi_{rm}) \,, \tag{3}$$

where the amplitudes σ_{rm} and phases φ_{rm} of a specific force-wave with spatial order r and temporal order m are determined by

$$\sigma_{rm} = \frac{1}{2} \cdot B_{\nu_1\mu_1} B_{\nu_2\mu_2}; \;\; \varphi_{rm} = \pi + \varphi_{\nu_1\mu_1} \pm \varphi_{\nu_2\mu_2}; \;\; r = \nu_1 \pm \nu_2; \;\; \omega_m = \omega_{\mu_1} \pm \omega_{\mu_2} \,. \tag{4}$$

Since the force excitations occur with these distinct ordinal numbers in space and in time, the vibration spectrum contains only those frequencies. The spatial ordinal numbers are also called mode numbers, since a force of mode r excites ideally only a vibration mode $m = r$. Low mode numbers are considered critically, because the stator system reacts comparatively soft for low mode numbers leading to larger deformations and thus acoustic radiation. Hence, most analytical models are based on the evaluation of such mode numbers. Force amplitudes can also be calculated analytically. For higher accuracy, the FEM is typically applied in 2D to solve MAXWELL's equations [3].

The $2p = 6$-pole induction machine under investigation has a rated mechanical power of 500 W. It has $N_1 = 36$ stator slots and $N_2 = 28$ rotor slots. The machine is operated at a constant 50 Hz grid as pump drive. The electromagnetic simulation and force calculation is performed using the *IEM*-inhouse software package *iMOOSE*.

3 Structural-dynamic simulation

After the electromagnetic simulation of the induction machine a structural-dynamic simulation is performed to determine the vibration. The surface-force density on the stator teeth obtained from the electromagnetic simulation is used as excitation. The vibration problem is formulated using HAMILTON's principle. After discretizing, the general vibration equation in frequency domain is obtained by

$$(\mathbf{K} + j\omega\mathbf{C} - \omega^2\mathbf{M}) \cdot \underline{\mathbf{d}}(\omega) = \underline{\mathbf{f}}(\omega) \,, \tag{5}$$

where $\mathbf{K}$, $\mathbf{C}$ and $\mathbf{M}$ are the global stiffness, damping and mass matrix, respectively. The imaginary number is denoted by j and ω describes the angular frequency of the problem. $\underline{\mathbf{d}}(\omega)$ is the vector of the complex nodal deformation, and $\underline{\mathbf{f}}(\omega)$ is the complex excitation force vector. As electrical machines can typically be considered as low damped systems [7], the term $j\omega\mathbf{C}$ is disregarded in this work.

The complex radial surface-force density $\underline{\sigma}(\omega = m\omega_0) = \sigma_{rm} \cdot e^{j\varphi_{rm}}$ is to be transformed from the electromagnetic simulation to a nodal force $\underline{\mathbf{f}}(\omega)$ on the mechanical model for each frequency, where ω_0 is the base frequency. Therefore, a unit force and a unit torque

$$\underline{\boldsymbol{\xi}}_{nr} = \int_{\Omega} \mathbf{e}_r(x) \cdot e^{jrx} N_n \,\mathrm{d}\Omega\,, \qquad \boldsymbol{\tau_n} = \frac{2}{\pi D^2 l_z} \int_{\Omega} \mathbf{e}_{\varphi}(x) N_n \,\mathrm{d}\Omega \tag{6}$$

are defined, respectively. The diameter of the stator bore is D and length of the active part of the machine is l_z. The nodal shape function of the FEM formulation is denoted N_n, and Ω is the stator inner surface domain at $r = D/2$. Then, the harmonic nodal force is determined by

$$\underline{\mathbf{f}}_n(\omega) = \sum_{r=-R}^{R} \underline{\sigma}_{rm} \cdot \underline{\boldsymbol{\xi}}_{nr} + \underline{T}_m \cdot \boldsymbol{\tau}_n\,, \tag{7}$$

where $\underline{T}_m$ is the complex amplitude of the m-th temporal order of the torque ripple. Force modes up to $R = 8$ are considered.

After a modal analysis using the software *Ansys*, the deformation is calculated applying a modal superposition

$$\underline{\mathbf{d}}(\omega) = \sum_{i=1}^{N} \frac{\boldsymbol{\Phi}_i^T \cdot \underline{\mathbf{f}}(\omega) \cdot \boldsymbol{\Phi}_i}{\omega_i^2 - \omega^2}\,, \tag{8}$$

where N is the number of eigenvalues and $\boldsymbol{\Phi}_i$ is the i-th mass-normalized eigenvector. The mechanical model of the induction machine under investigation is shown in Figure 1 together with the squared normal surface velocity on the housing simulated at 533 Hz. Since the machine is flange mounted, the boundary condition of the structural dynamic simulation is set, such that the displacement of the nodes around the mounting holes is zero.

4 Acoustic parameters of electrical machines

In order to analyze the acoustic performance and the noise emitted by electrical machines several acoustic parameters can be examined. During the design process reliable acoustic parameters that can be obtained in negligible additional time are required. This allows to seamlessly integrate acoustic aspects into the simulation process in the early design phase.

4.1 Mean-squared normal surface velocity

If the acoustic performance is to be directly evaluated by a vibrational analysis, the surface velocity is typically used as a parameter. It can be determined either at a fixed location, e.g. where an accelerometer may be placed, or as an integral quantity. Therefore, the mean-squared normal surface velocity is defined as

$$\overline{|v_n|^2} = \frac{1}{\Gamma} \int_{\Gamma} \|\underline{\mathbf{v}}_{\mathbf{n}}\|^2 \,\mathrm{d}\Gamma = \frac{1}{\Gamma} \int_{\Gamma} \underline{\mathbf{v}}_{\mathbf{n}}\, \underline{\mathbf{v}}_{\mathbf{n}}^{*} \,\mathrm{d}\Gamma, \tag{9}$$

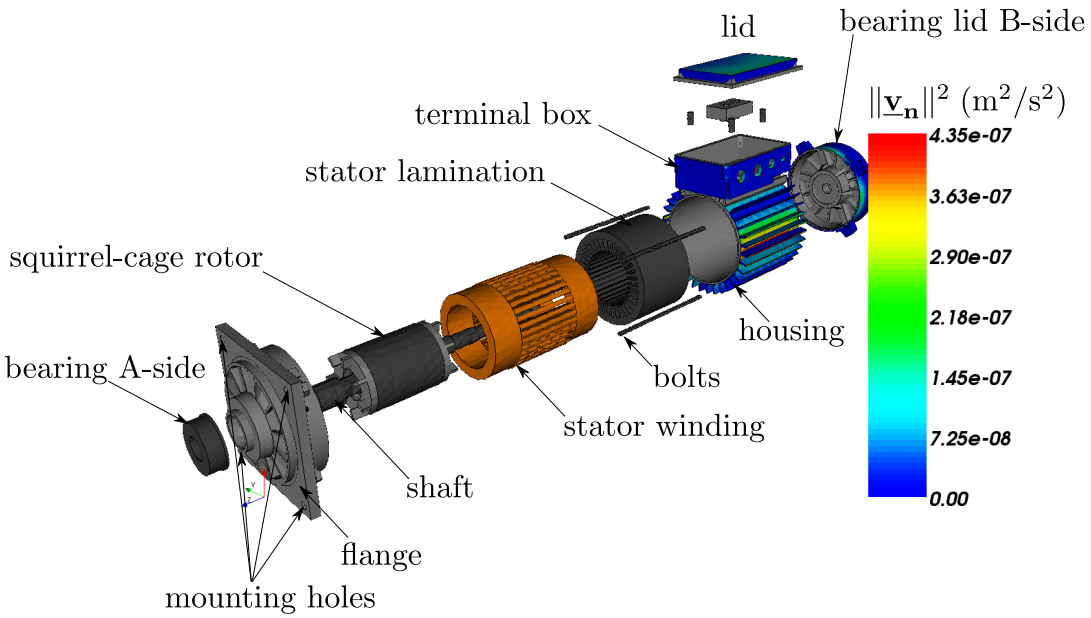

Figure 1: Mechanical model of the induction machine together with normal surface velocity on the housing at 533 Hz.

where the $\underline{\mathbf{v}}_\mathbf{n}^*$ denotes the complex conjugate function of $\underline{\mathbf{v}}_\mathbf{n}$ and Γ is the outer surface of the machine. The advantage of this parameter is that it can be determined immediately from the structural-dynamic simulation. In connection with a radiation model of a pulsating sphere it can be considered as an estimate for the radiated acoustic power, using the following equations

$$P = \frac{1}{2}\overline{|v_n|^2}\, W_\mathrm{s}, \qquad W_\mathrm{s} = \frac{\rho_0 c S}{1 + \frac{1}{k^2 a^2}}. \tag{10}$$

W_s is the radiation impedance for a pulsating sphere of radius a and surface S, k is the wavenumber and ρ_0 and c are the density and speed of sound in air, respectively. The radius is chosen in such a way that the surface of the sphere is approximately equal to the radiating surface of the machine. In the presented case, this leads to $a \approx 8\,\mathrm{cm}$. This model was used to determine the sound power level for the mean-squared velocity and the maximum squared velocity in Fig. 6.

4.2 Sound power

The sound power P and its level L_P are physical source parameters describing the acoustical behavior over frequency [8]. They are independent of the final scenario an object is used in. Together with the radiation pattern they build a source descriptor used e.g. for the prediction of sound propagation in complex acoustic scenarios. The sound power is defined as the surface integral over the normal component of the sound intensity vector $\mathbf{I}_\mathbf{w}$ as follows,

$$P = \int_S \mathbf{I}_\mathbf{w} \mathrm{d}\mathbf{S} = \int_S \frac{p^2}{\rho_0 c} \mathrm{d}S \tag{11}$$

where p is the sound pressure.

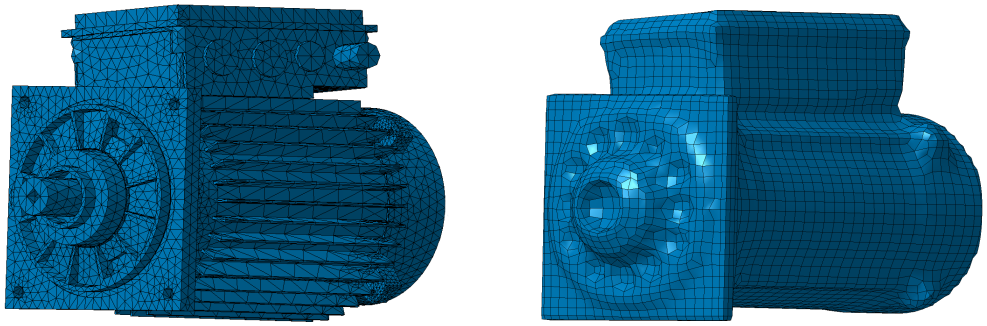

(a) Structural Mesh (b) Acoustic Mesh

Figure 2: Structural and acoustic mesh of the machine.

5 Acoustic Radiation

The sound radiation into the acoustic free-field can be calculated, for example by means of BEM simulation. In general, numeric simulations for detailed models and up to higher frequencies of approx. 5 kHz lead to intense and time-consuming calculations. A new approach is also used to shorten calculation times by using a trade-off between calculation time and precision.

5.1 BEM Simulation

The BEM is based on the numerical solution of the Helmholtz integral equation on the boundary surface of the investigated object [9]. While this computation is fairly complex and time-consuming, the precision that can be achieved is relatively high as effects of diffraction and reflection are included. The software used for all BEM simulations is *Virtual.Lab* Acoustics by *LMS*.

Often it is desirable to determine the sound radiation independently of the actual velocity distribution on the test object so that the result can be obtained quickly for many different load cases or – in the case of electrical machines – operating conditions. In *Virtual.Lab*, this is achieved by computing the so-called *Acoustic Transfer Vectors* (ATV) [10] that relate the volume velocity at each mesh node to the sound pressure at a specified set of field points. The post-processing step is then a simple vector multiplication with the surface velocity distribution and the superposition of the contribution of all nodes.

Since the computational cost rises with the element size, the very detailed model mesh that is used in the structural-dynamic analysis (Fig. 2a) has to be converted into a mesh for the acoustic radiation with the well-known six-elements-per-wavelength rule (Fig. 2b). For a maximum frequency of 5 kHz the average element size is chosen to be roughly 10 mm which results in a total number of 4257 nodes. Compared to the structural mesh with about 210000 nodes this is a factor 50 in size reduction. As the results for the surface velocity from the structural calculations are only available on the very fine mesh, a mapping of the data onto the acoustic mesh has to be performed. This is done using the mesh mapping function in *Virtual.Lab* which handles the connection between structural and acoustical nodes and applies a linear weighted sum in the case that multiple structural nodes affect the velocity at a single acoustic node.

The evaluation of the sound pressure is carried out at 38 field points of the *ISO Power Field Point Mesh* in *Virtual.Lab*. The field points are distributed on a unit sphere in such a way that it is divided

into equally-sized elements. From the simulated pressure at the field points the sound power can be calculated according to Eq. (11).

In terms of calculation times, the first step of processing the ATV, which only needs to be done once, is the more time-consuming part. For the model used in this study and the power field point mesh the processing time per frequency was roughly 4 minutes on a modern standard single-core computer. The post-processing that has to be performed for each load case takes less than a second per frequency, resulting in a total post-processing calculation time of 8 seconds for the 14 frequencies from the velocity input data.

5.2 Analytic solution for cylindrical geometry

The geometrical shape of the electrical machine can often be approximated by a cylinder, as it is the case for the given machine. Thus the far-field sound pressure can be estimated by an analytical cylinder radiation model from the surface velocity [11]. This model which has been applied frequently in research employs a finite cylinder with infinitely long stiffening baffles at each end and hence restricts vibrations to the dimensions of the machine [12, 13, 14]. As a consequence of the restricted velocity, end effects and the size of the machine can be taken into account.

Solving the wave equation in cylindrical coordinates and using EULER's equation one arrives at the following relation that describes the sound pressure in frequency domain as a function of the spatial velocity spectrum for exterior radiation problems:

$$p(r,\phi,z,\omega) = \frac{1}{2\,\pi} \sum_{n=-\infty}^{\infty} e^{jn\phi} \int_{-\infty}^{\infty} V_n(a,k_z) \frac{H_n(k_r r)}{H_n'(k_r a)} e^{jk_z} \mathrm{d}\, k_z. \tag{12}$$

Here, p is the sound pressure and V_n is the spatial radial velocity spectrum obtained from a double FOURIER transform of the velocity distribution. The index n donates the circumferential mode order of the velocity. H_n and H_n' are the HANKEL functions of n-th order and the derivation with regards to its argument, respectively. k_r and k_z are the wave numbers in radial and axial direction, a is the radius of the cylindrical machine. Due to the fact that the integration over k_z in Eq. (12) cannot be carried out and numerical solving methods have negative impact on the otherwise very fast calculation time (the main advantage of this approach), a technique called stationary phase approximation is used. It is explained in detail e.g. by WILLIAMS [11] and JUNGER [15] and is applicable for the far-field only. The result obtained from this method after a transform into spherical coordinates is the stationary phase point $k_z = k\cos(\theta)$ which eliminates the integral with regards to k_z and can be inserted into Eq. (12) yielding the following approximation for the sound pressure:

$$p(r,\phi,z) \approx \frac{\rho_0\, c}{\pi} \cdot \frac{e^{jkR}}{R} \sum_{n=-\infty}^{\infty} (-j)^n\, e^{jn\phi} \frac{V_n(a, k\cos(\theta))}{sin(\theta)\, H_n'(ka\sin(\theta))}. \tag{13}$$

Here the relation $k_r = \sqrt{k^2 - k_z^2}$ and the addition theorem $\sin(x)^2 + \cos(x)^2 = 1$ are applied. Eq. (13) allows to estimate the far-field sound pressure very quickly for a given velocity spectrum. This is the result from a two dimensional FOURIER transform of the velocity distribution on an ideal cylindrical surface.

The analytic model has been implemented in *MATLAB* by *Mathworks*. The surface velocity data has to be mapped to an equivalent perfect cylinder surface. Only the radial component of the surface velocity is significant for sound radiation. Mapping is done analogue to the procedure explained in

section 5.1. The mesh of the analytic cylinder is coarser than the acoustic mesh used in the BEM since no six-elements-per-wavelength rule has to be met. In the case of the machine examined it has 568 nodes which are equally spaced on the surface. Hence, there are 18 nodes in axial direction for a given angular ϕ and 32 nodes around the circumference for a given axial position.

The spatial velocity spectrum is obtained by means of a two-dimensional discrete FOURIER transform in z and ϕ direction. Since the velocity distribution is periodic in ϕ no error is induced through the spatial sampling as long as the highest circumferential mode order does not exceed half of the node number on a circumference of the cylinder (NYQUIST theorem). In axial direction zeros are added to the velocity distribution firstly to ensure a spatial restricted non-zero velocity and secondly to increase the resolution in the spectrum. The latter is necessary to reduce rounding error since the values of the velocity spectrum need to be found in Eq. (13) for certain values of k_z. As a consequence of the sampling in axial direction in combination with the spatially restricted velocity, aliasing will occur and hence induce some error. The number of samples in axial direction is determined by the highest axial vibration mode order that is expected to occur as well as by the maximum frequency that is of interest. The latter is a consequence of the stationary phase point which defines the highest spatial frequency in axial direction to be equal to the highest frequency of sound.

The main advantage of the analytic approach is the small requirements on computation power. For a given surface velocity the resulting sound radiation can be calculated more than 1000 times faster in comparison to the BEM, allowing convenient virtual prototyping within seconds of calculation including detailed radiation pattern not sound power only. Analytic calculation thus offers a fast method for predicting the sound radiation of a machine, even though it is an approximation due to the finite length of the cylinder and deviations from the perfectly cylindrical shape.

6 Results

The performance and applicability of the analytic cylinder model is evaluated by using BEM simulations for a perfect cylinder with the same geometry in both calculations and depicted in Figure 6. A random surface velocity distribution is used. Receiver points in 5 m distance are used to calculate the sound pressure. With the assumption of a far field, the sound power is calculated according to Eq. (11). As can be seen, the model performs well with only small deviations in sound power levels of approx. 1 dB.

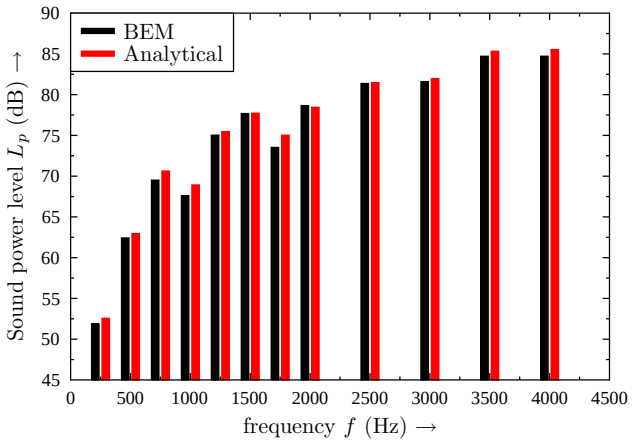

Figure 3: Comparison of analytical cylinder model and BEM simulation on perfect cylinder.

The comparison of the radiation pattern for the electrical machine for four different frequencies is

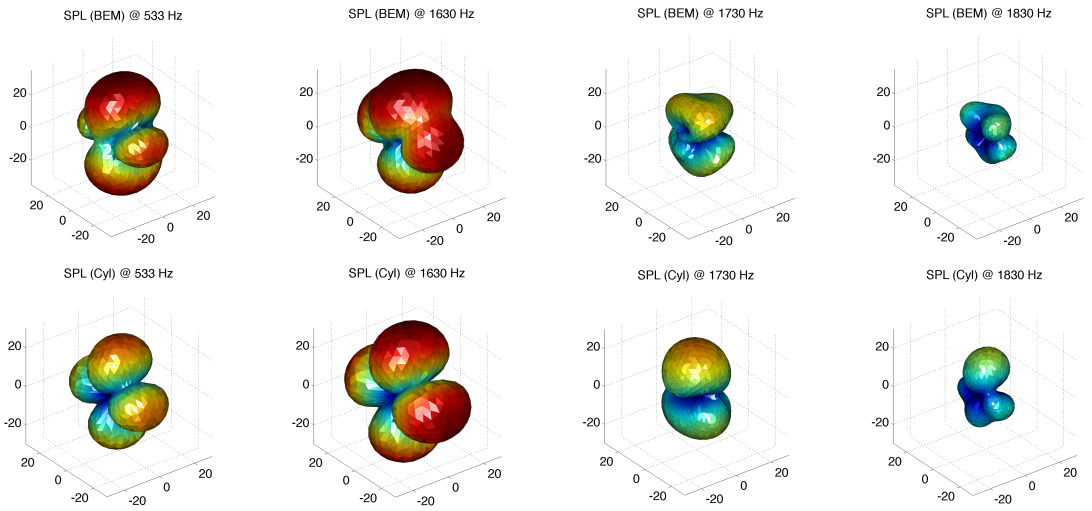

Figure 4: Comparison of radiation pattern for different frequencies obtained by BEM (top) and cylindrical harmonics (bottom).

shown in Figure 4. In the top row precise results from BEM simulations and in the bottom row the prediction by cylindrical harmonics calculation is shown, respectively. As can be seen, the shape of the radiation pattern can be fairly approximated by the analytical cylinder model. In z-direction differences occur due to the contribution in radiation of the end faces. As the machine is not a perfect cylinder errors in ϕ-direction are reasonable but not troublesome for the application. As a side effect of this calculation method radiation pattern analysis could also be integrated in the workflow for the machine design with only little more computational effort. The cylinder model is therefore applicable at least for the given machine.

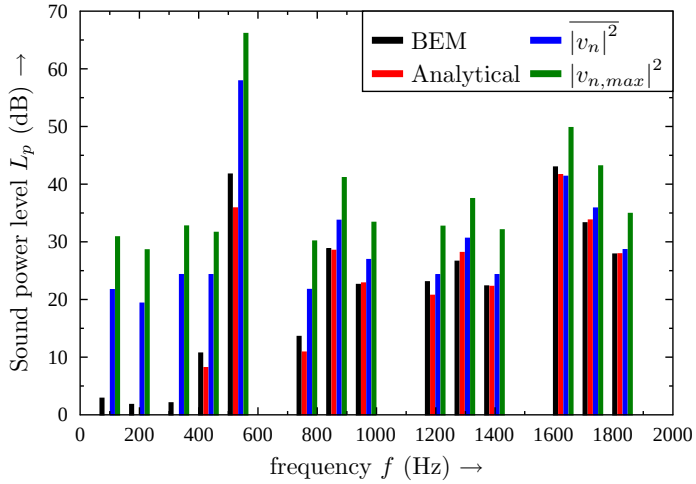

Figure 5: Comparison of acoustic scalar parameters for the induction machine.

In order to compare the performance of the acoustic design parameters, the estimated sound powers are plotted in Figure 6. As the machine only radiates at distinct frequencies only these frequencies are considered, e.g. at the calculated operation point, the machine vibrates at 533 Hz in a $r = 2$ mode, due to the first stator slot harmonic. The sound power is therefore not analyzed in fractional octave bands.

7 Conclusions and Future Work

The simulation procedure and basic calculus for the calculation of electrical machines up to their acoustic radiation based on CAD models have been introduced. Based on calculations for an exemplarily chosen machine, the parameters and different calculation models have been analyzed. The formerly used mean-squared surface velocity is directly accessible from electro-magnetic force calculation in conjunction with structural FEM simulations. The calculation time for this parameter is very short but it lacks of precise correlation to the actual acoustic performance. Nevertheless, it is a suitable parameter for a first prediction. The sound power level is a parameter directly related to the radiation of the machine and therefore preferable. As time consuming BEM simulations are commonly used to calculate the sound radiation, a different method using cylindrical decomposition has been proposed. This approach yields the sound pressure at arbitrary field points and sound power, being in good correlation with the precise results from BEM simulations. Hence, calculation times for the acoustic radiation can be significantly reduced. As the sound pressure is also in good agreement with the BEM results this clears the way for auralization applications.

As machines are generally designed to operate in different conditions, all conditions have to be simulated leading to long calculation times. In a future step, it will be tried to reduce calculations to a minimal set of significant simulation tasks in order to auralize electrical machines in computing time suitable for the design process. The results calculated and shown in this paper are already sufficient to auralize the airborne contribution of this machine for a specific load condition (torque/speed) e.g. inside a factory hall.

References

[1] H. Jordan, *Geräuscharme Elektromotoren*. W. Girardet, November 1950.

[2] J. Gieras, C. Wang, and J. C. Lai, *Noise of Polyphase Electric Motors*. CRC Press Taylor&Francis Group, 2006.

[3] C. Wang, J. Lai, and A. Astfalck, "Sound power radiated from an inverter driven induction motor II: Numerical analysis," *Electric Power Applications, IEE Proceedings*, vol. 151, pp. 341–348, May. 2004.

[4] S. Fingerhuth, P. Dietrich, M. Pollow, M. Vorländer, D. Franck, M. van der Giet, K. Hameyer, M. Bösing, K. A. Kasper, and R. W. De Doncker, "Towards the auralization of electrical machines in complex virtual scenarios," in *Tecniacústica Cádiz*, Spain, 2009.

[5] M. Vorländer, *Auralization – Fundamentals of Acoustics, Modelling, Simulation, Algorithms and Acoustic Virtual Reality*, RWTH edition ed. Springer-Verlag Berlin Heidelberg, 2008.

[6] F. Henrotte and K. Hameyer, "A theory for electromagnetic force formulas in continuous media," *Magnetics, IEEE Transactions on*, vol. 43, no. 4, pp. 1445–1448, April 2007.

[7] S. J. Yang, *Low-noise electrical motors*. Clarendon Press Oxford, 1981.

[8] F. Fahy, *Sound Intensity*. Elsevier Applied Sciences, 1995.

[9] A. J. Burton and G. F. Miller, "The Application of Integral Equation Methods to the Numerical Solution of Some Exterior Boundary-Value Problems," *Proceedings of the Royal Society of London. Series A, Mathematical and Physical Sciences (1934-1990)*, vol. 323, no. 1553, pp. 201–210, 1971.

[10] F. Gerard, M. Tournour, N. El Masri, L. Cremers, M. Felice, and A. Selmane, "Acoustic transfer vectors for numerical modeling of engine noise," *Journal of Sound and Vibration*, vol. 36, no. 7, pp. 20–25, 2002.

[11] E. G. Williams, *Fourier Acoustics: Sound Radiation and Nearfield Acoustical Holography*. Academic Press, 1999.

[12] C. Wang and J. Lai, "The sound radiation efficiency of finite length acoustically thick circular cylindrical shells under mechanical excitation I: Theoretical analysis," *Journal of Sound and Vibration*, no. 2, 2000.

[13] H. Lee and R. Singh, "Comparison of two analytical methods used to calculate sound radiation from radial vibration modes of a thick annular disk," *Journal of Sound and Vibration*, vol. 285, 2005.

[14] Z. Zhu and D. Howe, "Improved methods for prediction of electromagnetic noise radiated by electrical machines," *Electric Power Applications, IEE Proceedings* -, vol. 141, no. 2, pp. 109–120, 1994.

[15] M. Junger and D. Feit, *Sound, structures, and their interaction*. MIT Press, 1986.